Structures and Reaction Mechanisms of Propene Oxide Isomerization on H-ZSM-5: An ONIOM Study

Supawadee Namuangruk,[†,‡] Pipat Khongpracha,[†,‡] Piboon Pantu,[†,‡] and Jumras Limtrakul,*[,†,‡]

Laboratory for Computational and Applied Chemistry, Department of Chemistry, Faculty of Science, Kasetsart University, Bangkok 10900, Thailand; and Center of Nanotechnology, Kasetsart University Research and Development Institute, Kasetsart University, Bangkok 10900, Thailand

Received: August 15, 2006; In Final Form: October 18, 2006

The isomerization mechanisms of propene oxide over H-ZSM-5 zeolite have been investigated via the utilization of 5T and 46T cluster models calculated by the B3LYP/6-31G(d,p) and the ONIOM(B3LYP/6-31G(d,p): UFF) methods, respectively. The reactions are considered to proceed through a stepwise mechanism: (1) the epoxide ring protonation, and concurrently the ring-opening, and (2) the 1,2-hydride shift forming the adsorbed carbonyl compound. Because of the asymmetric structure of propene oxide, two different C−O bonds (more or less substituted carbon atom sides) can be broken leading to two different types of products, propanal and propanone. The ring-opening step of these mechanisms is found to be the rate-determining step with an activation barrier of 38.5 kcal/mol for the propanal and of 42.4 kcal/mol for the propanone. Therefore, the propanal is predicted to be the main product for this reaction.

Introduction

Epoxides are important intermediates for organic synthesis and for the chemical and petrochemical industries. With their high ring constraint, epoxides are very reactive, giving them extensive use for the syntheses of complex organic compounds, polymers, and macromolecules[1−4] via the ring-opening and isomerization reactions. Numerous experimental and theoretical studies have investigated the reactions and mechanisms of the ring-opening isomerization, the isomerization of epoxides in solutions with and without acid catalysts and catalytic enzymes.[5−15] The isomerization of unsymmetrical epoxides can give two different carbonyl compounds. For example, isomerization of propene oxide produces propanal and propanone. The major product is propanal, which results from the breaking of the more sterically hindered C−O bond of the epoxide ring. For chemical processes, these reactions were conventionally catalyzed by Lewis acid catalysts ($AlCl_3$, and BF_3, etc.) that are highly toxic and corrosive and, consequently, present a serious waste disposal problem. To substitute the conventional catalysts to reduce these problems, solid catalysts, for example, Al_2O_3, Al_2O_3−SiO_2, ZnO[16] Nafion-H,[12] zeolites,[10] and so forth, have been developed. Among these solid catalysts, zeolites are considered to be one of the most promising alternatives because they can be reused and reactivated. Moreover, their nanoscaled pore size can be used as a high selectivity microreactor for a desired product. Acidic zeolites are active in the isomerization of propene oxide. The reactions occur on Brønsted or Lewis acid sites. The confined environment of zeolites also favors the dimerization. The product distributions strongly depend on the pore sizes of the zeolites.[10]

Zeolites are microporous aluminosilicates with a large number of atoms in the unit cell. To obtain more manageable sizes for the ab initio calculations, small clusters representing the catalytic active site have been studied in the past. However, this has meant that the essential confinement effect created by the part of the surrounding framework has been neglected. In earlier theoretical studies, it was deemed sufficient to investigate only the reaction mechanisms of small clusters using first-principle calculations on the reactions of small- and medium-size adsorbates. However, those clusters precluded consideration of the electrostatic and van der Waals effects of the zeolite framework, which significantly affect the stability of the intermediates and transition states. It is important, therefore, that the larger clusters which include such potential be taken into consideration. To facilitate this, the large quantum clusters and periodic calculations have been specifically developed. However, even though these calculations do provide accurate results, they are really prohibitive in terms of computational time and expense. The more recent development of hybrid methods, such as the embedded cluster or combined quantum mechanics/molecular mechanics (QM/MM),[17−22] and our-own-N-layered integrated molecular orbital + molecular mechanics (ONIOM)[23−25] methods, have made it possible to successfully describe the confinement effect from the zeolite wall as well and at a much more economical computational cost.

Recent studies[17,26−30] have shown the necessity to include in investigations the significant effects that the zeolite framework contributes to the interaction and reaction mechanisms over zeolite between the adsorbate molecule and the zeolite wall. In this work, we use the ONIOM method, which has been successfully employed to describe the effect of the zeolite framework[23,31,32] and which reveals the importance of the van der Waals interaction from the zeolite framework in the nature of the reaction over the zeolite catalyst but the interaction is neglected in a small quantum cluster.

To the best of our knowledge, no theoretical study related to the isomerization of epoxides over zeolites has been reported. In this work, we present the theoretical reaction mechanisms of the propene oxide isomerization over H-ZSM-5 zeolite. Two

* Author to whom correspondence should be addressed. E-mail: jumras.l@ku.ac.th.
† Laboratory for Computational and Applied Chemistry.
‡ Center of Nanotechnology.

10.1021/jp065266s CCC: $33.50
Published on Web 12/21/2006

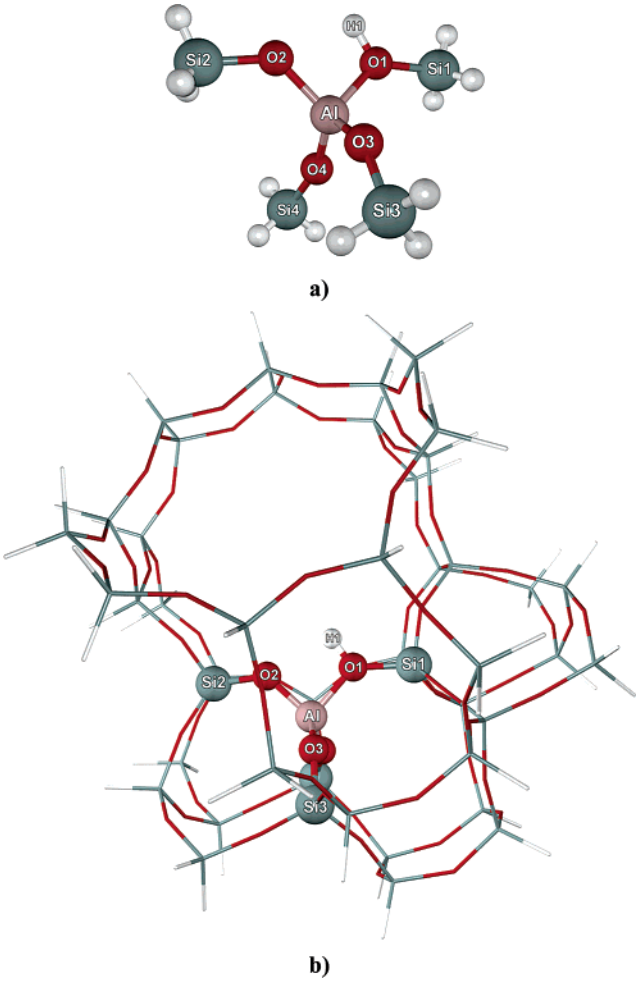

Figure 1. The 5T and 46T clusters represent the active site of ZSM-5 zeolite in the zigzag channel view. The ball-and-stick graphics illustrates the relaxed geometry resulting from calculations at B3LYP/6-31G(d,p), the lines from the universal force field (UFF).

different products, propanal and propanone, are formed by the breaking of different C−O bonds. The mechanisms start from the ring-opening of propene oxide coordinated to the acidic proton of zeolite to form the intermediate, processing via the carbenium-like ion as the transition state, followed by a 1,2-hydride shift between the adjacent carbon atom to form the carbonyl compounds. With the aim of describing the effect of the zeolite framework on this reaction, we have discussed the results obtained from the 46T cluster, including the zeolite framework which is treated by an ONIOM method, and we have compared those with the ones obtained from the smaller 5T quantum cluster. In the Results and Discussion section, we relate the details of the energetics and structural stabilities affected from the zeolite framework.

2. Models and Methods

The active site of H-ZSM-5 zeolite was represented by two different cluster sizes: 5T and 46T clusters, which are shown in Figure 1. The first model consists of five tetrahedral atoms $[(H_3SiO)_3Al(OH)SiH_3]$ which are located at the cross section of the straight channel and zigzag channel and are consequently considered as the active region that allows the adsorbate molecules to react with the Brønsted proton. In this cluster, all atoms except the dangling hydrogen atoms, which are constrained in Si−O directions in the framework of the ZSM-5 zeolite, including the adsorbate molecules, are fully relaxed to replicate the real reaction phenomena. The second cluster was modeled by the two-layered ONIOM model. During the optimization, only the 5T regions $[(\equiv SiO)_3Al(OH)Si\equiv]$ with the adsorbate molecules are allowed to relax since it has been pointed out that full relaxation of zeolite clusters can lead to structures that deviate largely from the experimental zeolite geometries.[30] This model has also been validated in our previous studies[31−32] and also in this study to give reasonable adsorption energies which compared well with the experimental measured values. The ONIOM scheme has been implemented on the extended 46T cluster model to represent the zeolite pore cavity and zeolite framework, which includes the 10-membered ring channel containing the active region (represented as balls and sticks in Figure 1), as in the 5T cluster. The consequence of this is that the results obtained are anticipated to clarify the effect of the zeolite framework.

All the calculations were performed by the Gaussian 03 program.[33] The adsorbate molecules and 5T cluster of the first model, as well as the 5T region of the ONIOM model, were treated by the B3LYP[34−36] density functional theory at 6-31G-(d,p), while the rest of the framework is treated with the universal force field (UFF).[37]

TABLE 1: The Optimized Geometric Parameters of the Zeolite 5T and 46T Clusters Calculated at B3LYP/ 6-31G(d,p) and ONIOM(B3LYP/6-31G(d,p):UFF) Levels[a]

parameters	5T	46T
	Distances	
O1−H1	0.969	0.970
Al−O1	1.853	1.786
Al−O2	1.703	1.656
Al−O3	1.687	1.637
Al−O4	1.687	1.649
Si1−O1	1.694	1.670
Si2−O2	1.620	1.592
Si1−O3	1.627	1.597
Si2−O4	1.615	1.574
	Angles	
∠Si1O1Al	131.6	132.4
∠Si2O2Al	130.0	131.5
∠Si3O3Al	135.3	134.9
∠Si4O4Al	151.8	143.8

[a] Distances are in angstroms and angles are in degrees.

3. Results and Discussion

3.1. The Zeolite Models and Adsorption Complexes. The 5T and 46T clusters are shown in Figure 1 while their geometric parameters are tabulated in Table 1. To observe the catalytic framework effect on the reaction over the active site, the atoms in the 5T region in both clusters have been optimized with the exception of the atoms in the extended framework of the ONIOM model, which were fixed. Comparison of the 5T quantum cluster and the 46T ONIOM model reveals little difference in the geometric parameters. As the extended framework has only a small effect on the active site geometry by decreasing the Brønsted acid angle (Al−O1−Si1) by about 1° and slightly lengthening the O1−H1 bond distance, the indication is that the active site in the 46T ONIOM model might be more acidic than that in the 5T quantum cluster, which, in turn, leads to the prediction that the adsorption energy of adsorbates on the ONIOM model should also be higher.

The adsorption complexes of the propene oxide, propanal and propanone, which are the reactant and products for the isomerization of propene oxide, on the Brønsted acid site of the ZSM-5 zeolite in the quantum cluster and ONIOM model are depicted in Figure 2. These adsorbates interact on the acidic proton of

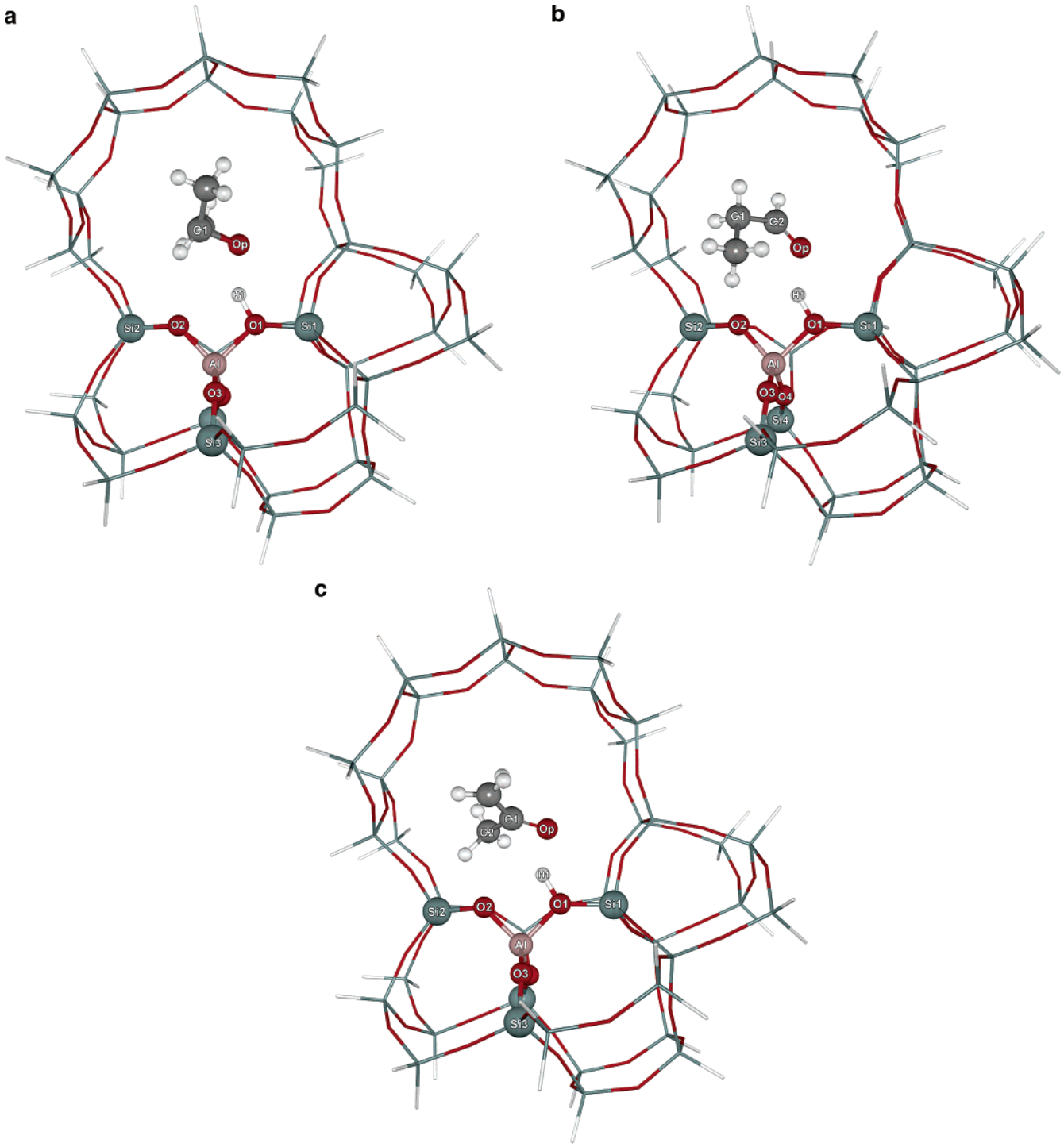

Figure 2. Presentation of models of ZSM-5 and its interaction with adsorbates: ONIOM2 layer models of 46T cluster interacts with (a) propene oxide, (b) propanal, and (c) propanone.

zeolite via hydrogen bonding, and the geometric structures of all adsorption complexes are slightly deviated from those of isolated structures (Table 2).

In the propene oxide adsorption complex (Figure 2a), the oxygen atom of propene oxide interacts with the acidic proton via hydrogen bonding with the Op−H1 distance of 1.540 Å (cf. Table 2). The hydrogen bonding interaction lengthens the Brønsted acid O1−H1 bond distance by 0.054 Å. Although the epoxide ring is asymmetric, the epoxide ring center aligns above the acidic site with almost equal distances of C1−O1 and C2−O1 and C1−O2 and C2−O2. Because of the decrease of the electron density on Op via the electron transfer from the Op to the H1 atom, the C1−Op and C2−Op bonds are elongated by 0.026 and 0.015 Å, respectively. The greater increase in the length of the C1−Op bond leads to the prediction that it would be broken more easily than the shorter C2−Op bond. The adsorption energy is evaluated to be −16.8 and −30.8 kcal/mol for the 5T quantum cluster and ONIOM calculations, respectively.

The propanal and propanone also adsorb on the acidic proton of zeolite via hydrogen bonding (see Figure 2b and 2c). Since the carbonyl C═Op bonds are strong double bonds, they are not changed significantly during the adsorption on the active site of zeolite. The C═Op bond of the propanone adsorption complex alters slightly from isolated propanone by 0.017 Å, and that of the propanal is changed by only 0.008 Å (cf. Table

TABLE 2: The Relevant Parameters for the Propene Oxide, Propanal, and Propanone Adsorbed on 5T and 46T H-ZSM-5 Zeolite Clusters

	distances (Å)					
	O1−Hz	Op−Hz	C2−Op	C1−C2	C1−Op	adsorption energies (kcal/mol)
isolated propene oxide			1.434	1.470	1.435	
propene oxide on 5T	1.023	1.533	1.452	1.468	1.464	−16.8
propene oxide on 46T	1.023	1.540	1.449	1.468	1.461	−30.8
isolated propanal			1.211	1.512	2.419	
propanal on 5T	1.004	1.614	1.222	1.498	2.435	−15.0
propanal on 46T	1.015	1.585	1.225	1.493	2.416	−26.3
isolated propanone			2.394	1.520	1.216	
propanone on 5T	1.025	1.527	2.393	1.506	1.232	−16.7
propanone on 46T	1.039	1.476	2.400	1.506	1.233	−30.4[a]

[a] The propanone (acetone) adsorption on H-ZSM-5 from experimental data is −31.1 kcal/mol.[38]

2). The hydrogen bonding interaction lengthens the Brønsted acid O1−H1 bond distance by 0.046 and 0.068 Å for the adsorption of propanal and propanone, respectively. The adsorption energies of propanal and propanone are evaluated to be −15.0 and −16.7 kcal/mol for the quantum cluster and −26.3 and −30.4 kcal/mol for the ONIOM model, respectively. The framework effect in the ONIOM model approximately doubles the adsorption energies of the adsorption complexes. The van der Waals interactions between the adsorbates and the zeolite pore walls stabilize the adsorption complexes inside.

The calculated adsorption energy of propanone of −30.4 kcal/mol compares well with the experimental data of −31.1 kcal/mol.[38] This result indicates that the combination between the B3LYP density functional theory at the active region and UFF force field at the extended framework in the ONIOM model can produce reasonable interaction energies between these adsorbates and the zeolite catalyst. Therefore, this ONIOM model should be suitable to use for investigation of the isomerization reaction for this system.

3.2. The Reaction Mechanism of Isomerization of Propene Oxide. The isomerization mechanism of propene oxide to carbonyl compounds is considered to occur via the C−O bond breaking of the oxirane ring in the propene oxide molecule. The asymmetric structure of propene oxide has two different C−O bonds (more or less substituted carbon atom sides) that can be broken and, thus, has two possible products of the ring-opening reaction: propanal and propanone. Propanal is formed via the C−O bond breaking at the tertiary carbon atom (C1−Op), while propanone is formed via the C−O bond breaking at the other carbon atom (C2−Op) in the oxirane ring (cf. Figure 2). To elucidate the explanation and represent it in a more instructive format, the detailed mechanism will be separated into two subsections.

A. The Reaction Mechanism Leading to Propanal. The isomerization mechanism of propene oxide to propanal on H-ZSM-5 zeolite has been proposed as a stepwise reaction processes. The calculated energy profile for the isomerization of propene oxide to propanal is shown in Figure 3a and the calculated relative energies and activation energies are shown in Table 3. First, the propene oxide molecule diffuses into the pore of zeolite and then adsorbs on the acidic proton at the active site to form the propene oxide adsorption complex. Propene oxide adsorbs on the acidic proton via hydrogen bonding with the Op−H1 distance of 1.540 Å and the adsorption energy of −30.8 kcal/mol. In this adsorption complex, the C1−Op and C2−Op bond lengths are calculated to be 1.461 Å and 1.449 Å, respectively. Then, the C1−Op bond is broken to produce the secondary alkoxide intermediate (Int_A) through the secondary carbenium ion transition state (TS1_A). At the TS1_A transition-state configuration, the acidic proton of the zeolite is protonated to the adsorbed propene oxide, the C1−Op bond is broken, and the hybridization of C1 is changed from tetrahedral (sp^3) to planar (sp^2). The transition state (cf. Figure 3b) can be confirmed by the frequency calculation with one imaginary frequency at −224.8 cm^{-1}, which is related to the movement of the acidic proton of zeolite (H1) to the propene oxide oxygen (Op) and the breaking of C1−Op bond. The calculated energy barrier for this ring-opening step is 38.5 kcal/mol and the apparent activation energy is 7.7 kcal/mol. The secondary alkoxide intermediate (Int_A) is attached to the oxygen atom (O2) of the zeolite and is stabilized by the zeolite framework.

The next step is the carbonyl-forming step, which involves the transformation of the Int_A intermediate to the adsorbed propanal (P_A) via the 1,2-hydride shift. At this transition-state configuration (TS2_A), the H2 atom is moving toward the carbon atom C2 placed with the C2−H2 and C1−H2 distances being 1.190 Å and 1.654 Å, respectively. The H1 atom is located in-between the O1 and Op atoms with Op−H1 = 1.023 Å and H1−O1 = 1.552 Å. Figure 3c depicts the vibrational motion that occurs at the TS2_A transition state which possesses one imaginary frequency at −770.6 cm^{-1}. This movement corresponds to the H2 atom transfer from C1 to C2 simultaneously with the C1−O2 covalent bond breaking and the H1 transfer from Op back to O1 to restore the active site of the zeolite. The activation energy for this step is calculated to be 18.2 kcal/mol and the propanal product is adsorbed on the acidic site of the ZSM-5 zeolite with the adsorption energy of −48.1 kcal/mol. Finally, the adsorbed propanal is desorbed endothermically and requires an energy of 26.3 kcal/mol.

Previously, Coxon et al.[7] studied the isomerization of protonated propene oxide to protonated propanal and reported that the reaction followed the concerted asynchronous mechanism. The authors observed that the hydride migration did not occur until the ring-opening step was completed, although the authors did not find the carbenium ion intermediate. However, for the isomerization of protonated methyl propene oxide, the authors were able to find the more stable tertiary carbenium ion intermediate and reported that the reaction was stepwise.[9] In this study, the reaction takes place inside the zeolite pore environment. Although the zeolite does not directly protonate the propene oxide, the hydrogen bonding interaction with the zeolite helps to facilitate the ring-opening reaction. Moreover, the adjacent O2 atom of the zeolite can help to stabilize the ring-opening intermediate carbenium ion by forming the stable alkoxide intermediate as it has been observed that surface alkoxide species are important reaction intermediates in many reactions in zeolites.[39−41]

Although all geometric parameters calculated from the quantum cluster (written in parentheses in Figure 3a) are quite similar to those obtained from the ONIOM model, the calculated

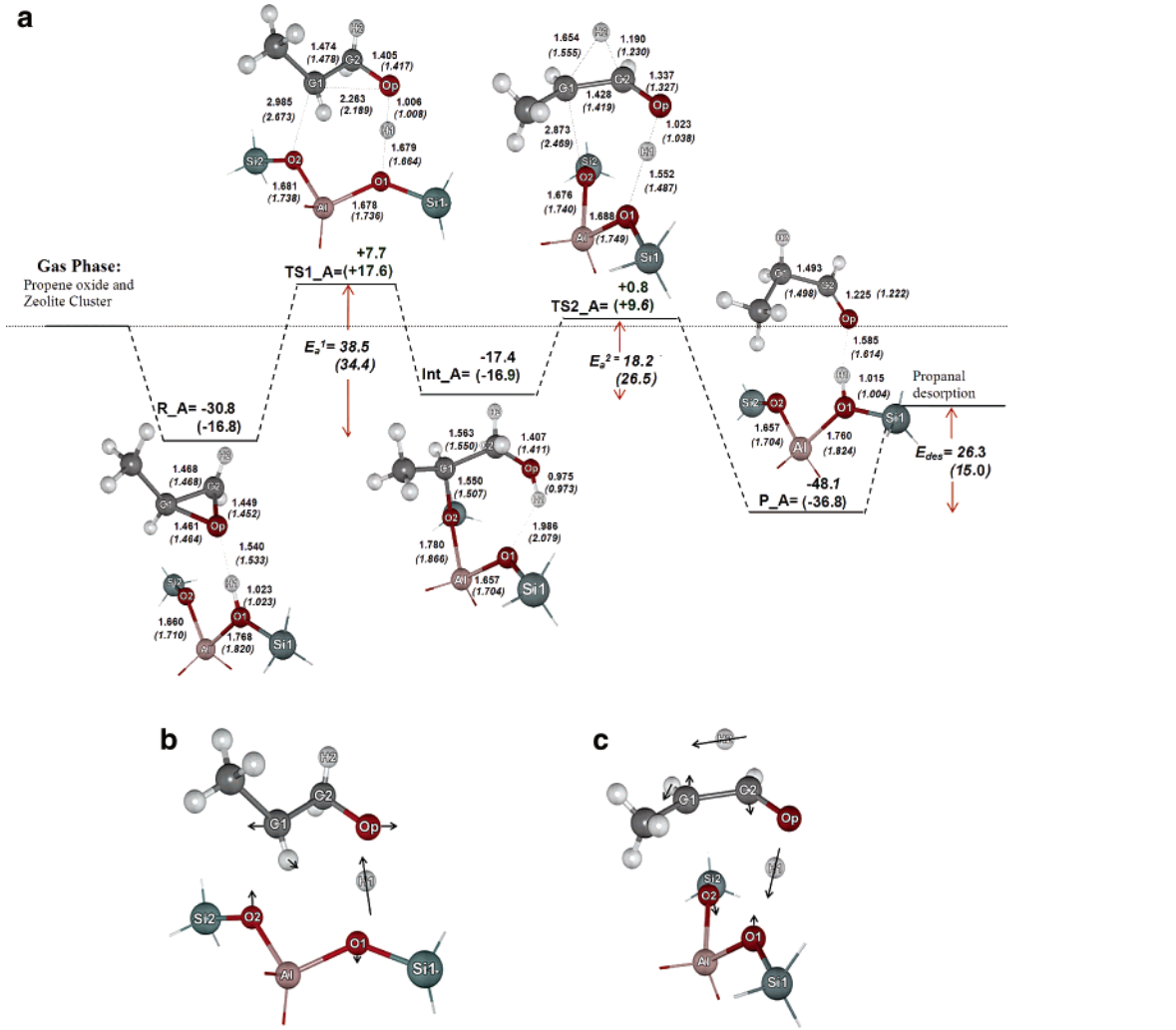

Figure 3. (a) The calculated energy profile for the isomerization of propene oxide to propanal over 46T and 5T (in parentheses) clusters; (b) the vibrational movement corresponding to the imaginary frequency at the TS1_A; (c) the vibrational movement corresponding to the imaginary frequency at the TS2_A.

relative energies and energy barriers differ considerably from the ONIOM results. It may seem surprising that the ONIOM and the cluster calculations give almost the same relative energy for the alkoxide intermediate (Int_A). This is derived by the erroneous prediction of relative stability of the alkoxide species by the cluster calculation. Since the structure of the small cluster can be significantly changed to accommodate the formation of the alkoxide, the alkoxide species can form a stronger covalent bond to the zeolite cluster. The covalent C−O bond distance in the cluster calculation is 1.507 Å which is shorter than the C−O bond of 1.550 Å in the case of the ONIOM model, and the zeolite O2AlO1 angle is 95.8 degrees in the cluster model while the O2AlO1 angle is 96.5 degrees in the ONIOM calculations. As a result, the covalent bond stabilization of the alkoxide in the small cluster is overestimated. The influence of the local geometry of zeolite on the stability of alkoxide intermediates has been extensively discussed by Boronat et al.[42] Thus, it is indicated that a small quantum cluster can predict only the geometrical characters of the stationary points along the reaction pathway. However, for the energetic profile of the reaction, the ONIOM approach that takes into account the zeolite framework effects should be more suitable. The cause of these differences between the two models is the van der Waals effect from the zeolite framework acting on the adsorbate species at each stationary point.

TABLE 3: The Calculated Relative Energies (kcal/mol) of Reactant, First-Transition State (TS1), Intermediate, Second-Transition State (TS2), Product, First Activation Energy Barrier (ΔE_a^1), and Second Activation Energy Barrier (ΔE_a^2) for the Isomerization Reaction of Propene Oxide over 5T and 46T Clusters of H-ZSM-5 Calculated at B3LYP/6-31G(d,p) and ONIOM(B3LYP/6-31G(d,p):UFF) Levels

	5T cluster		46T cluster	
	propanal	propanone	propanal	propanone
reactant	−16.8	−16.8	−30.8	−30.8
TS1	17.6	24.5	7.7	11.6
intermediate	−16.9	−21.6	−17.4	−24.5
TS2	9.6	7.8	0.8	−1.3
product	−36.8	−46.3	−48.1	−60.0
product des.	−15.0	−16.7	−26.3	−30.4
ΔE_a^1	34.4	41.3	38.5	42.4
ΔE_a^2	26.5	29.4	18.2	23.2

B. The Reaction Mechanism Leading to Propanone. The isomerization of propene oxide can also produce propanone by breaking the less substituted C−O bond at the ring-opening step. The calculated energy profile for this route is illustrated in Figure 4a. The reaction starts with the adsorbed propene oxide (R_B) on the acidic proton of the zeolite. Subsequently, an adsorbed propene oxide is protonated at the Op atom and the less substituted C2−Op bond is broken leading to the formation of the primary alkoxide intermediate through the transition-state TS1_B, which possesses a primary carbenium ion configuration,

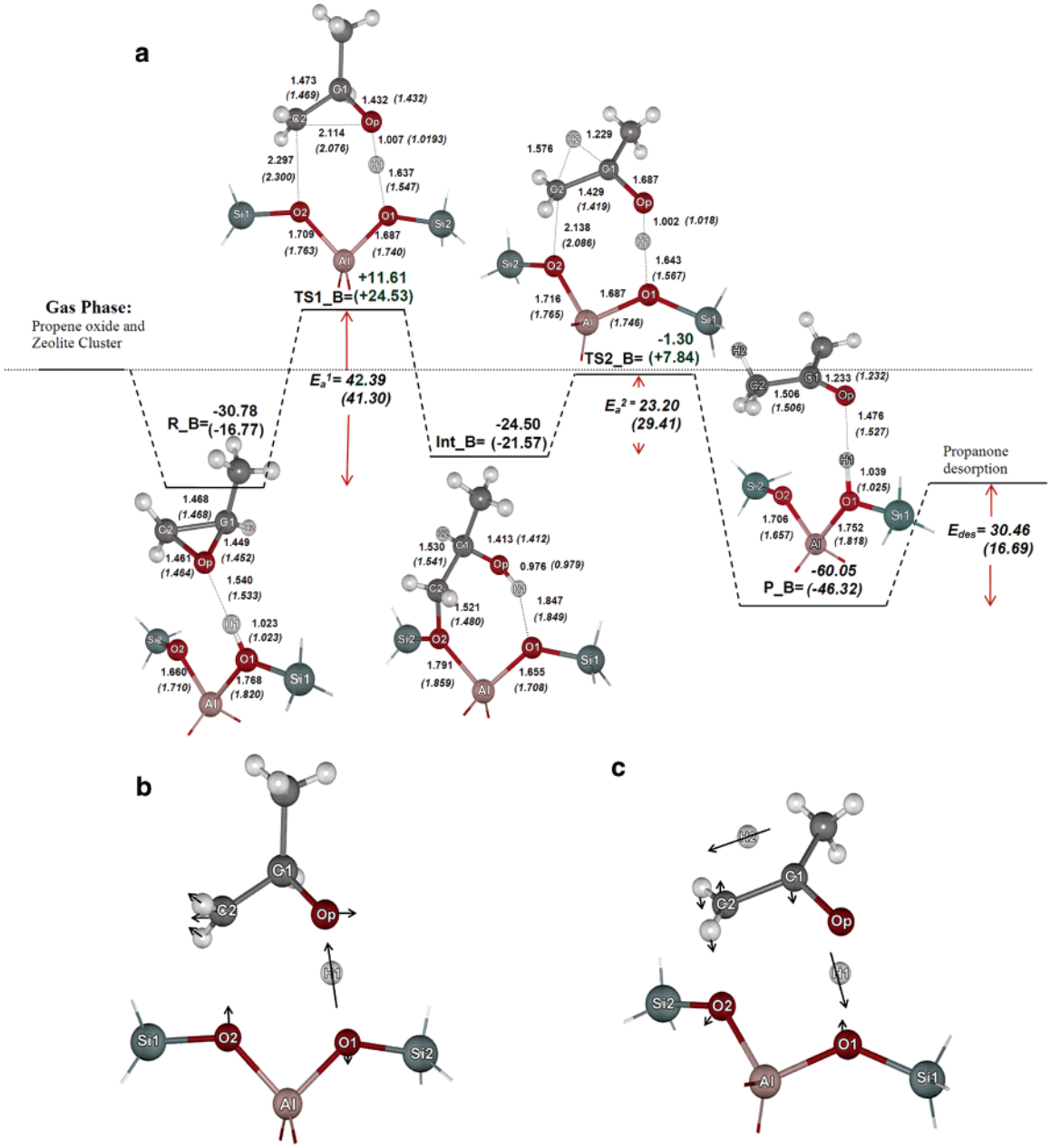

Figure 4. (a) The calculated energy profile for the isomerization of propene oxide to propanone over 46T and 5T (in parentheses) clusters; (b) the vibrational movement corresponding to the imaginary frequency at the TS1_B; (c) the vibrational movement corresponding to the imaginary frequency at the TS2_B.

which is less stable than the secondary carbenium ion (TS1_A) in the propanal route. This justification has been supported by the higher calculated energy barrier and apparent energy for the primary carbenium ion (TS1_B) which is evaluated to be 42.4 and 11.6 kcal/mol, respectively. The transition-state TS1_B has been verified by one imaginary frequency at -389.7 cm^{-1}, which involves the following movement (Figure 4b): the acidic proton transfers from the zeolite framework to the oxygen atom of propene oxide and the C2−Op bond breaks simultaneously as the covalent bond between C2 and O2 forms. At the transition-state configuration, it is observed that a H1 atom moves from O1 close to Op with the Op−H1 distance of 1.007 Å and the O1−H1 distance of 1.637 Å.

The binding energy of the primary alkoxide intermediate (Int_B) is calculated to be 24.5 kcal/mol, which is more stable than that of the secondary alkoxide intermediate (Int_A) by 7.1 kcal/mol, resulting from the less steric disturbance effect from the substituted group on the alkoxide carbon atom. This less steric hindrance on the alkoxide carbon atom allows the adsorbate to move closer to the active site of the zeolite in comparison to the more steric one, C2−O2 = 1.521 Å for the primary alkoxide (Int_B) and C1−O2 = 1.550 Å for the secondary alkoxide (Int_A), respectively. Therefore, in the zeolite framework, the less steric alkoxide (Int_B) is more stable than the more steric alkoxide (Int_A). This observation is also in agreement with previous reports that the stability of the alkoxide intermediate formed in the zeolite structure is very sensitive to the local geometry of the active site and the nature of the alkoxide carbon atom.[42−44] When the degree of substitution on alkoxide carbon increases, the covalent C−O bond distance is lengthened and the alkoxide is destabilized.[42]

The primary alkoxide intermediate (Int_B) is transformed to the adsorbed propanone product (P_B) via the 1,2-hydride shift process through the transition state (TS2_B) which indicates that the distance of the breaking of the C1−H2 bond is 1.229 Å, the forming of the C2−H2 bond is 1.576 Å, while the

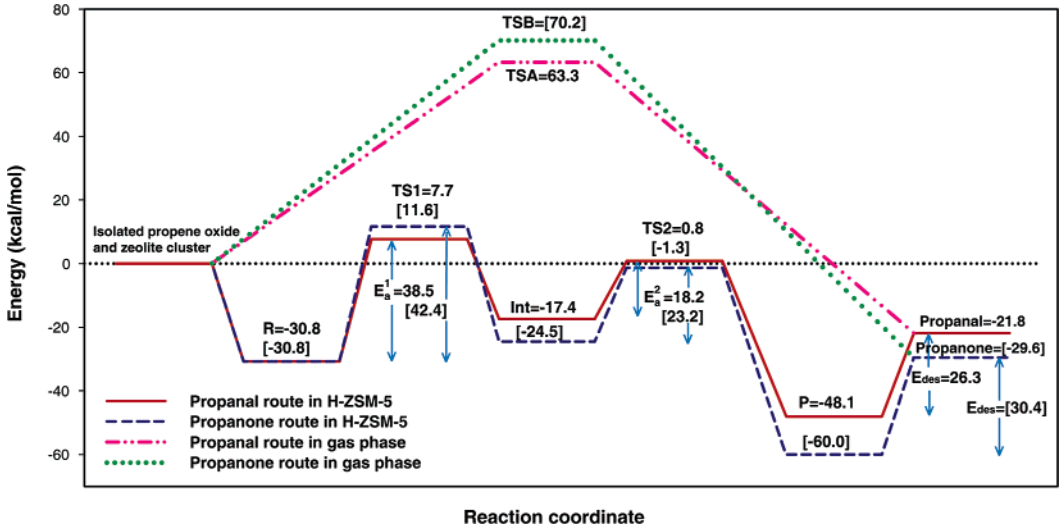

Figure 5. The energy profile of the isomerization of propene oxide to propanal on H-ZSM-5 zeolite (solid line), to propanone on H-ZSM-5 zeolite (dash line) calculated at ONIOM(B3LYP/6-31G(d,p):UFF), to propanal in gas phase (dash dot dot line), and to propanone in gas phase (dot line) calculated at B3LYP/6-31G(d,p).

breaking C2−O2 covalent bond is lengthened from 1.521 to 2.138 Å. Consequently, H1 moves back to the bridging oxygen atom by locating midway between Op and O1. The O1−H1 bond is shorter than Op−H1 bond, 1.039 and 1.476 Å, respectively. This vibrational movement, which corresponds to the imaginary frequency at −861.5 cm^{-1}, is depicted in Figure 4c. The energy barrier is calculated to be 23.2 kcal/mol, which is higher than that of the propanal route by 5.0 kcal/mol. Finally, the adsorbed propanone is desorbed endothermically, requiring a desorption energy of 30.4 kcal/mol.

For ease of comparison, the complete energetic profiles for all mechanisms are shown in the same diagram (Figure 5). This diagram shows the energies obtained from the ONIOM model which include the zeolite framework effect and the gas-phase noncatalyzed isomerizations for comparison. Without a catalyst, the gas-phase propene oxide isomerization occurs via a single concerted step with high reaction barriers of 63.3 and 70.2 kcal/mol for the formation of propanal and propanone, respectively. It is undoubtedly observed that H-ZSM-5 zeolite alters the propene oxide isomerization mechanism to go through a series of steps with lower reaction barriers. The reaction starts with propene oxide adsorbed on the acid proton of zeolite. The ring-opening step is considered to be the rate-determining step. The activation energies are 38.5 and 42.4 kcal/mol for propanal and propanone formation, respectively. The reaction intermediates and transition states are greatly stabilized by the zeolite framework. The transition states of this rate-determining step only lie above the reactants by 7.7 and 11.6 kcal/mol for propanal and propanone formation, respectively. The step following is the energy barrier for carbonyl forming, which involves the 1,2-hydride shift on connecting the C−C bond, and is evaluated to be 18.2 and 23.2 kcal/mol for propanal and propanone, respectively. Therefore, it can be concluded, by considering the relative reaction barrier and the transition-state stability, that the propanal is more favorably formed than the propanone. However, since the confinement effect of the H-ZSM-5 zeolite stabilizes the transition states and intermediates for both routes, the preference against the rupture of the more sterically hindered C−O bond is not very high. This finding corresponds well with the experimental results[10] that propanal was produced in a higher yield than that of propanone but the minor product, propanone, was also produced in a significant yield for the propene oxide isomerization in H-ZSM-5 zeolites.

Conclusion

The isomerization of propene oxide over 5T and 46T clusters of H-ZSM-5 zeolite has been investigated by using the B3LYP/6-31G(d,p) and ONIOM(B3LYP/6-31G(d,p):UFF) methods. The reaction mechanisms proceed through a ring-opening step followed by a 1,2-hydride shift to form two different carbonyl compounds, propanal and propanone. The ring-opening step of these mechanisms is found to be the rate-determining step and their transition states are in the carbenium ion form. The propanal route proceeds via the secondary carbenium ion while that of the propanone proceeds via the primary one. Because the sterically more hindered C−O bond can be broken more easily and the secondary carbenium ion transition state is more stable, the ring-opening activation barrier for the propanal of 38.5 kcal/mol is lower than that for the propanone of 42.4 kcal/mol. The main product from this reaction is, therefore, the propanal.

The computational results suggest that the 5T cluster is adequate to determine the geometrical characters of the transition state, the intermediate, the reactant, and the product of these small adsorbates. However, since the 5T cluster does not take into account the van der Waals from the zeolite framework, it cannot give reasonable results for the energetic profile of the reaction. The extended 46T ONIOM model, which includes the zeolite cavity and those effects, can be used to calculate more reliable results.

Acknowledgment. This work was supported in part by grants from the Thailand Research Fund through the Senior Research Scholar to J.L. and the Royal Golden Jubilee Ph.D. Program (3.C.KU/48/A.1) to S.N. The Kasetsart University Research and Development Institute (KURDI) and the Ministry of University Affairs under the Science and Technology Higher Education Development Project (MUA-ADB funds) are also acknowledged, as is the support from the National Nanotechnology Center (NANOTEC, Thailand).

References and Notes

(1) Katsuki, T.; Sharpless, K. B. *J. Am. Chem. Soc.* **1980**, *102*, 5974−5976.
(2) Smith, J. G. *Synthesis* **1984**, 629−656.
(3) Cheng, Z.; Zhu, X.; Fu, G. D.; Kang, E. T.; Neoh, K. G. *Macromolecules* **2005**, *38*, 7187−7192.

(4) Carlier, P. R. *Angew. Chem., Int. Ed.* **2004**, *43*, 2602−2605.
(5) George, P.; Bock, C. W.; Glusker, J. P. *J. Phys. Chem.* **1992**, *96*, 3702−3708.
(6) Dimitrova, R.; Minkov, V.; Micheva, N. *Appl. Catal. A* **1996**, *145*, 49−55.
(7) Coxon, J. M.; Maclagan, R. G. A. R.; Rauk, A.; Thorpe, A. J.; Whalen, D. *J. Am. Chem. Soc.* **1997**, *119*, 4712−4718.
(8) Laitinen, T.; Rouvinen, J.; Peraekylae, M. *J. Org. Chem.* **1998**, *63*, 8157−8162.
(9) Coxon, J. M.; Thorpe, A. J. *J. Org. Chem.* **1999**, *64*, 9575−9586.
(10) Fasi, A.; Gomory, A.; Palinko, I.; Kiricsi, I. *J. Catal.* **2001**, *200*, 340−344.
(11) Lau, E. Y.; Newby, Z. E.; Bruice, T. C. *J. Am. Chem. Soc.* **2001**, *123*, 3350−3357.
(12) Fasi, A.; Palinko, I.; Gomory, A.; Kiricsi, I. *J. Mol. Catal. A* **2004**, *208*, 307−311.
(13) Helten, H.; Schirmeister, T.; Engels, B. *J. Phys. Chem. A* **2004**, *108*, 7691−7701.
(14) Helten, H.; Schirmeister, T.; Engels, B. *J. Org. Chem.* **2005**, *70*, 233−237.
(15) Carlier, P. R.; Deora, N.; Crawford, T. D. *J. Org. Chem.* **2006**, *71*, 1592−1597.
(16) Molnar, A.; Bucsi, I.; Bartok, M.; Resofszki, G.; Gati, G. *J. Catal.* **1991**, *129*, 303−306.
(17) Braendle, M.; Sauer, J. *J. Am. Chem. Soc.* **1998**, *120*, 1556−1570.
(18) Greatbanks, S. P.; Hillier, I. H.; Burton, N. A.; Sherwood, P. *J. Chem. Phys.* **1996**, *105*, 3770−3776.
(19) Limtrakul, J.; Jungsuttiwong, S.; Khongpracha, P. *J. Mol. Struct.* **2000**, *525*, 153−162.
(20) Treesukol, P.; Lewis, J. P.; Limtrakul, J.; Truong, T. N. *Chem. Phys. Lett.* **2001**, *350*, 128−134.
(21) Khaliullin, R. Z.; Bell, A. T.; Kazansky, V. B. *J. Phys. Chem. A* **2001**, *105*, 10454−10461.
(22) Hillier, I. H. *THEOCHEM* **1999**, *463*, 45−52.
(23) Solans-Monfort, X.; Bertran, J.; Branchadell, V.; Sodupe, M. *J. Phys. Chem. B* **2002**, *106*, 10220−10226.
(24) Dapprich, S.; Komiromi, I.; Byun, K. S.; Morokuma, K.; Frisch, M. J. *THEOCHEM* **1999**, *461−462*, 1−21.
(25) Svensson, M.; Humbel, S.; Froese, R. D. J.; Matsubara, T.; Sieber, S.; Morokuma, K. *J. Phys. Chem.* **1996**, *100*, 19357−19363.
(26) Yang, L.; Trafford, K.; Kresnawahjuesa, O.; Sepa, J.; Gorte, R. J.; White, D. *J. Phys. Chem. B* **2001**, *105*, 1935−1942.
(27) Sinclair, P. E.; de Vries, A.; Sherwood, P.; Catlow, C. R. A.; van Santen, R. A. *J. Chem. Soc., Faraday Trans.* **1998**, *94*, 3401−3408.
(28) Derouane, E. G.; Chang, C. D. *Microporous Mesoporous Mater.* **2000**, *35−36*, 425−433.
(29) Vos, A. M.; Rozanska, X.; Schoonheydt, R. A.; van Santen, R. A.; Hutschka, F.; Hafner, J. *J. Am. Chem. Soc.* **2001**, *123*, 2799−2809.
(30) Brand, H. V.; Curtiss, L. A.; Iton, L. E. *J. Phys. Chem.* **1993**, *97*, 12773−12782.
(31) Namuangruk, S.; Pantu, P.; Limtrakul, J. *J. Catal.* **2004**, *225*, 523−530.
(32) Namuangruk, S.; Pantu, P.; Limtrakul, J. *ChemPhysChem* **2005**, *6*, 1333−1339.
(33) Frisch, M. J.; Trucks, G. W.; Schlegel, H. B.; Scuseria, G. E.; Robb, M. A.; Cheeseman, J. R.; Montgomery, J. A., Jr.; Vreven, T.; Kudin, K. N.; Burant, J. C.; Millam, J. M.; Iyengar, S. S.; Tomasi, J.; Barone, V.; Mennucci, B.; Cossi, M.; Scalmani, G.; Rega, N.; Petersson, G. A.; Nakatsuji, H.; Hada, M.; Ehara, M.; Toyota, K.; Fukuda, R.; Hasegawa, J.; Ishida, M.; Nakajima, T.; Honda, Y.; Kitao, O.; Nakai, H.; Klene, M.; Li, X.; Knox, J. E.; Hratchian, H. P.; Cross, J. B.; Bakken, V.; Adamo, C.; Jaramillo, J.; Gomperts, R.; Stratmann, R. E.; Yazyev, O.; Austin, A. J.; Cammi, R.; Pomelli, C.; Ochterski, J. W.; Ayala, P. Y.; Morokuma, K.; Voth, G. A.; Salvador, P.; Dannenberg, J. J.; Zakrzewski, V. G.; Dapprich, S.; Daniels, A. D.; Strain, M. C.; Farkas, O.; Malick, D. K.; Rabuck, A. D.; Raghavachari, K.; Foresman, J. B.; Ortiz, J. V.; Cui, Q.; Baboul, A. G.; Clifford, S.; Cioslowski, J.; Stefanov, B. B.; Liu, G.; Liashenko, A.; Piskorz, P.; Komaromi, I.; Martin, R. L.; Fox, D. J.; Keith, T.; Al-Laham, M. A.; Peng, C. Y.; Nanayakkara, A.; Challacombe, M.; Gill, P. M. W.; Johnson, B.; Chen, W.; Wong, M. W.; Gonzalez, C.; Pople, J. A. *Gaussian 03*, revision B.05; Gaussian, Inc.: Wallingford, CT, 2004.
(34) Becke, A. D. *J. Chem. Phys.* **1993**, *98*, 5648−5652.
(35) Lee, C.; Yang, W.; Parr, R. G. *Phys. Rev. B* **1988**, *37*, 785−789.
(36) Stephens, P. J.; Devlin, F. J.; Chabalowski, C. F.; Frisch, M. J. *J. Phys. Chem.* **1994**, *98*, 11623−11627.
(37) Rappe, A. K.; Casewit, C. J.; Colwell, K. S.; Goddard, W. A., III; Skiff, W. M. *J. Am. Chem. Soc.* **1992**, *114*, 10024−10035.
(38) Sepa, J.; Lee, C.; Gorte, R. J.; White, D.; Kassab, E.; Evleth, E. M.; Jessri, H.; Allavena, M. *J. Phys. Chem.* **1996**, *100*, 18515−18523.
(39) Nieminen, V.; Sierka, M.; Murzin, D. Y.; Sauer, J. *J. Catal.* **2005**, *231*, 393−404.
(40) Geobaldo, F.; Spoto, G.; Bordiga, S.; Lamberti, C.; Zecchina, A. *J. Chem. Soc., Faraday Trans.* **1997**, *93*, 1243−1249.
(41) Lesthaeghe, D.; Van Speybroeck, V.; Marin, G. B.; Waroquier, M. *J. Phys. Chem. B* **2005**, *109*, 7952−7960.
(42) Boronat, M.; Zicovich-Wilson, C. M.; Viruela, P.; Corma, A. *J. Phys. Chem. B* **2001**, *105*, 11169−11177.
(43) Boronat, M.; Viruela, P. M.; Corma, A. *J. Am. Chem. Soc.* **2004**, *126*, 3300−3309.
(44) Boronat, M.; Viruela, P.; Corma, A. *J. Phys. Chem. A* **1998**, *102*, 9863−9868.